ACS SENSORS

Article

pubs.acs.org/acssensors

Design and Application of an Optical Sensor for Simultaneous Imaging of pH and Dissolved O_2 with Low Cross-Talk

Maria Moßhammer,[†,‡] Martin Strobl,[‡] Michael Kühl,[†,∥] Ingo Klimant,[‡] Sergey M. Borisov,*[,‡] and Klaus Koren*[,†]

[†]Marine Biological Section, Department of Biology, University of Copenhagen, 3000 Helsingør, Denmark

[‡]Institute of Analytical Chemistry and Food Chemistry, Graz University of Technology, 8010 Graz, Austria

[∥]Plant Functional Biology and Climate Change Cluster, University of Technology Sydney, Ultimo, New South Wales 2007, Australia

Supporting Information

ABSTRACT: Visualization and quantification of analytes such as O_2 or pH is essential in biological research. Here we present the design and application of a new optical dual-analyte sensor for imaging, optimized to have low cross-sensitivity between the two analytes O_2 and pH. The used indicator and reference dyes were selected to match the different channels of a commercial 2CCD (RGB + NIR) camera. A red-light emitting O_2-sensitive europium complex ($Eu(HPhN)_3dpp$) with a dynamic range of 0−20% O_2 in the finished sensor was combined with a near-infrared emitting pH indicator (OHButoxy-aza-BODIPY) with a dynamic range of pH 7.2−8.8. To enable ratiometric readout, an inert reference coumarin dye (Bu_3Coum) was co-immobilized with the optical indicators. In order to maximize the sensor signal, inert diamond powder was added to one sensor layer as a simple way to increase scattering of light within the sensor. Furthermore, the addition of an optical isolation layer enabled measurements in highly fluorescent samples, such as algal biofilms. The sensor was tested in a marine photosynthetic microbial mat.

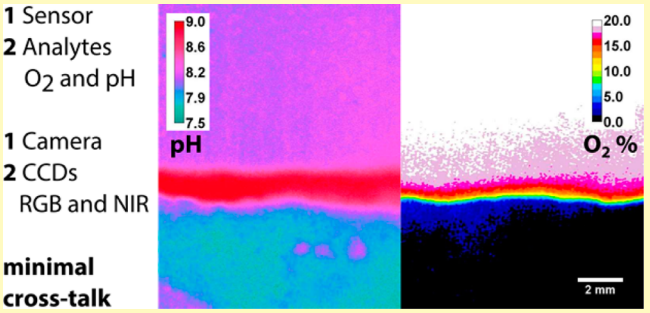

KEYWORDS: *dual-analyte sensor, chemical imaging, biofilm, microbial mat, sensor application*

Optical sensors based on reversible changes in luminescence of specific indicators allow the measurement[1] as well as the visualization[2] of analyte concentrations in a variety of formats. Fiber optical based sensors enable point measurements with high spatial resolution,[3] whereas planar sensor optodes[4] allow the imaging and analysis of larger areas. In environmental sciences the application of planar optical sensors has, e.g., enabled new experimental studies of the composition and function of marine sediments,[5−7] microbial mats,[8] plant rhizospheres,[9,10] biofilms,[11,12] and photosynthetic microbes.[13]

Planar optodes can be imaged by three commonly used methods. The simplest, but at the same time most error-prone, method is intensity-based imaging,[14,15] where the analyte-dependent change in sensor luminescence intensity is converted into an analyte concentration. This method is very sensitive to structural inhomogeneity, i.e., variable indicator concentrations in the planar optode or fluctuations in either the light source or detector (camera) including uneven excitation of the planar optode. In comparison, ratiometric imaging gives a more robust readout of luminescence-based sensors.[16−19] In this imaging mode a second analyte-independent emission from a reference dye is measured alongside the analyte-dependent emission form the optical indicator dye. Most artifacts due to sensor heterogeneity and uneven illumination can be compensated by calculating ratios between the inert emission and the analyte-dependent emission. Even more robust measurements with planar optodes can be obtained by luminescence lifetime-based imaging,[4,20,21] where an intrinsically referenced analyte-dependent parameter is measured.[22] However, lifetime imaging involves the use of rather specialized and expensive imaging setups[23] and is suitable mostly for optical oxygen and temperature probes. Lifetime based imaging of fluorescent probes (e.g., pH sensors) showing an "on−off" characteristic is hardly possible. Ratiometric imaging, on the contrary, can be carried out for many different analytes even using relatively simple commercial color cameras,[16,24] where the Bayer color filter on the camera chip enables the separation of the incident light into the three primary colors: blue, green, and red. Therefore, ratiometric images can be generated by simply comparing the images of the different color channels without the need of using multiple filters or light sources. Due to the simplicity and low cost of such RGB-camera based approaches, ratiometric, chemical imaging is currently gaining popularity within many different fields.[16,18,24−26]

Received: February 1, 2016
Accepted: April 8, 2016
Published: April 8, 2016

DOI: 10.1021/acssensors.6b00071
ACS Sens. 2016, 1, 681−687

In order to enable the imaging of two or more chemical parameters simultaneously, multiple indicators can be combined within a single optode.[17,25,27] Common RGB color cameras can in principle be used to read out two indicator dyes and one reference dye. However, such readout of dual analyte sensors with RGB color cameras is limited by the spectral overlap of the green channel with the two other channels, potentially causing cross-sensitivity between the individual sensor readouts. In addition, the choice of indicators and references is limited, as if excitations takes place in the blue region and all three channels are reserved for indicators and the reference, it is very difficult to separate the emission and the excitation in the blue region. A simple way to expand the potential of ratiometric readout is to use a 2CCD camera,[17] where the incoming light is split equally onto a normal RGB camera chip and an additional near-infrared (NIR) sensitive camera chip. This adds an extra spectral window for combining reference and indicator dyes and allows the use of NIR emitting indicators.

In this study we used a similar 2CCD imaging setup in combination with a new dual sensor system for simultaneous imaging of pH and O_2 with minimal cross-sensitivity between the two analytes. In order to achieve this low cross-sensitivity an appropriate combination of indicators and sensor materials had to be found. We describe the rationale behind the sensor design, sensor manufacturing, and calibration along with a practical application for studying O_2 dynamics and pH dynamics simultaneously in a complex photosynthetic microbial mat with high intrinsic fluorescence from photopigments.

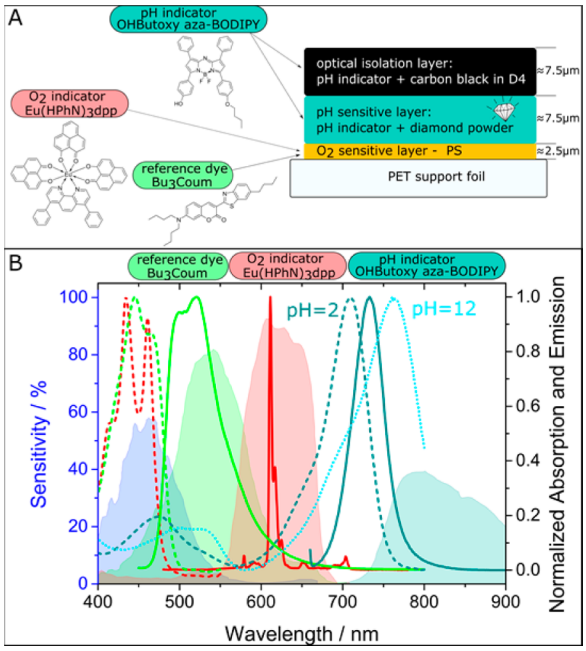

Figure 1. (A) Schematic drawing of the new optical O_2 and pH dual sensor composed of a three layer system containing the depicted indictor and reference dyes. (B) Spectra of the dyes (absorption in dashed and emission in solid lines). The spectral sensitivity of the four channels in the dual CCD camera is also shown (filled spectra colored according to the spectral range).

EXPERIMENTAL SECTION

Materials. The used indicator dyes OHButoxy-aza-BODIPY[28] and $Eu(HPhN)_3dpp$[29] were synthesized according to published methods (see Figure 1 for chemical structures). Polyurethane hydrogel (Hydromed D4) was obtained from AdvanSource biomaterials (advbiomaterials.com). Polystyrene (PS, MW 250 000) was bought from ACROS Organics (acros.com). Monocrystalline diamond powder was purchased from Microdiamant (microdiamant.com). All buffer materials (acetic acid, MES, TRIS, and CAPS) as well as 2-propanol and toluene were purchased from ROTH (carlroth.com). NaCl was obtained from AnalaR NORMAPUR – VWR (de.vwr.com/store/) chemicals, and carbon black was purchased from KREMER (kremer-pigmente.de). The PET support foil was obtained from Goodfellow (goodfellow.com). All chemicals were used as received.

Synthesis of the Reference Dye. Bu_3Coum was synthesized analogously to the literature procedure[30] (Supporting Information Figure S1). Briefly, 4-dibutylamino-2-hydroxybenzaldehyde prepared from 3-dibutylaminophenol[31] was condensed with 2-(6-butylbenzo-[*d*]thiazol-2-yl)acetonitrile (prepared from 6-butyl-2-benzothiazole-amine via 2-amino-5-butylbenzenethiol) to give an iminocoumarin that was converted to coumarin via treatment with HCl and was then further purified on column chromatography (silica-gel).

2-Amino-5-butylbenzenethiol. ^{1}H NMR ($CDCl_3$, 300 MHz): 6.97 (m, 2H), 6.65 (d, 1H), 4.0–3.5 (m, 3H), 2.38 (t, 2H), 1.44 (quint, 2H), 1.28 (m, 2H), 0.88 (t, 3H).

2-(6-butylbenzo[d]thiazol-2-yl)acetonitrile. ^{1}H NMR (DMSO-d_6, 300 MHz): 7.47 (s, 1H), 7.40 (s, 2H), 7.24 (d, 1H), 7.03 (d, 1H), 2.58 (t, 2H), 1.55 (quint, 2H), 1.29 (m, 2H), 0.90 (t, 3H).

Bu_3Coum. ^{1}H NMR ($CDCl_3$, 300 MHz): 8.96 (s, 1H), 7.95 (d, 1H), 7.72 (s, 1H), 7.48 (d, 1H), 7.31 (d, 1H), 6.64 (d, 1H), 6.53 (s, 1H), 3.37 (t, 4H), 2.76 (t, 2H), 1.63 (m, 6H), 1.38 (m, 6H), 0.99 (m, 9H). NMR spectra in Supporting Information Figures S1–S5.

Camera Setup. The setup used consisted of a JAI AD-080 GE 2CCD Multispectral camera (jai.com) equipped with a Schneider KREUZNACH objective (1.4/23 CCTV-LENS 400–1000 nm; schneiderkreuznach.com). A 510 nm long-pass filter (OG 510 Schott) was placed in front of the objective and an additional plastic filter (#10 medium yellow from leefilters.com) was placed in front of the long-pass filter to reduce the fluorescence of the glass filter and the background. The sensor can be illuminated with UV or blue LEDs (400–470 nm); we used a high power 405 nm LED (LedEngin purchased from rs-online.com) with a custom-built LED trigger (National instruments USB 6008 and an adequate power supply). Image acquisition and triggering of the LED was done with a custom-made software from Bioras Aps (bioras.com); the software is available from the authors upon request. Camera settings for the RGB chip were 0.3 s exposure time and a receiver gain of 30, and for the NIR chip the exposure time was 0.3 s and the receiver gain 90.

Sensor Preparation. For the O_2 sensitive layer, 1 mg of the Eu-complex and 0.15 mg of the coumarin reference dye were dissolved in 1.67 g 12%w/w solution of PS (in toluene). The solution was knife coated on a dust free PET film yielding a ~2.5-μm-thick layer after solvent evaporation.

For the pH sensitive layer, 0.05%w/w (0.5 mg) of the OHButoxy-aza-BODIPY was dissolved in 250 μL THF and added to 1 g of a 10.0% w/w solution of D4 (isopropanol:water, 9:1 w/w) containing 10.0% w/w (100 mg) diamond powder, serving as a signal enhancer. The dispersion was knife coated on top of the O_2 sensitive layer yielding a ~7.5-μm-thick pH sensitive layer after solvent evaporation.

For the optical isolation layer, 1.00% w/w (10 mg) of carbon black was dispersed in 1 g 10.0% w/w solution of D4 (isopropanol: water, 9:1 w/w). 0.05%w/w (0.5 mg) of the OHButoxy-aza-BODIPY dissolved in 250 μL THF was added. The dispersion was knife coated on top of the pH sensitive layer yielding a ~7.5-μm-thick optical isolation after solvent evaporation. The total thickness of the final dual-analyte sensor with optical isolation was thus <20 μm.

Sensor Calibration and Characterization. A dual sensor foil area of approximately 6 × 3 cm^2 was taped on the inside of a transparent flow chamber with a glass wall that was also used to study the microbial mat (see below) and imaging was done from the side. For calibration the pH of water in the flow chamber was adjusted using different buffers (MES, TRIS, phosphate, all at a concentration of 20 mM and a salinity of 30 PSU, equaling the used seawater). Oxygen

DOI: 10.1021/acssensors.6b00071
ACS Sens. 2016, 1, 681–687

levels were altered with the help of compressed O_2 and N_2, which were mixed by a PC-controlled gas mixer (sensor-sense.nl) prior to flushing the water in the flow chamber. The calibrations and the experiment were performed at the same constant temperature (22.5 ± 0.5 °C). The chamber was sealed at both ends during calibration. Temperature and O_2 levels were also monitored with a quicksilver thermometer and a fiber-optic O_2 meter (Piccolo2 equipped with a dipping probe; Pyroscience GmbH, Aachen Germany; pyro-science.com), respectively.

Image Analysis. The acquired images were split into the red, green, blue, and NIR channels and analyzed using the freely available software ImageJ (rsbweb.nih.gov/ij/) using the freely available plugins "Stack Sorter" and "Ratio Plus". In order to obtain O_2 and pH concentration images, the following steps were performed: For O_2, the red channel (O_2 sensitive emission of the Eu-complex) and green channel (emission of the coumarin reference dye) images were divided; For pH, the NIR (pH sensitive emission of the OHButoxy-aza BODIPY) and green channel (emission of the coumarin reference dye) images were divided. From these ratio images, the mean values and standard deviations were measured using ImageJ and plotted against the analyte concentration. This yielded calibration curves for O_2 and pH, respectively, that were fitted with an exponential decay function (O_2) or a sigmoidal function (pH) using OriginPro9.2 (originlab.com). Based on these calibrations, experimental ratio images from the biological measurements were transferred to chemical images in ImageJ using the curve fit functions; as ImageJ does not support sigmoidal fits, a linear fit to the pH-dependent ratios between pH 7 and 9 was used (Figure 2).

Sampling of Microbial Mat and Measurement of O_2 and pH Dynamics. Sediment colonized by a dense biofilm of phototrophic microorganisms, i.e., microbial mats were collected from sheltered, sandy areas at the coast of Limfjorden, near Aggersund, Denmark (57°00′02.15N, 9°17′12.89E). The sampling site is exposed to changes in sea level resulting from winds, causing it to be exposed to air, desiccated, or flooded for time periods between hours and weeks.[32,33] However, there are only minor influences due to tides.[33] The intermittent desiccation inhibits grazing animals and the top layer of the sediment is densely populated by filamentous cyanobacteria[34] and other microorganisms.

Sediment samples were collected in August 2015 using small (8 × 5 × 2 cm^3) plexiglass boxes. The sampling boxes were cut in half and taped together prior to sampling. The samples were kept under air-saturated seawater and light exposure for at least 24 h before conducting experiments. For the dual imaging, the tape was removed and the samples cut in half and immediately pressed against the calibrated dual sensor in the flow chamber, in order to avoid oxidation of the cut surface (see Supporting Information for picture of the sampling box and the cut samples). The flow chamber was flooded with seawater (from a 10 L reservoir kept at a constant temperature 22.5 ± 0.5 °C) and the sample was illuminated vertically from above using a halogen lamp equipped with a collimating lens (KL-2500, Schott GmbH) providing an incident downwelling irradiance (400–700 nm) of 330 μmol photons m^{-2} s^{-1} for 30 min; incident light was quantified with an underwater quantum irradiance meter (ULM-500, WALZ, walz.com). Image collection started immediately after the light was switched off and pictures were taken every 30 s for 30 min. Pictures of the sample cross section were taken after the experiment under ambient and UV illumination. Those pictures were used together with the O_2 images to define the sample surface.

RESULTS AND DISCUSSION

The aim of this study was to design an optical dual-analyte sensor with minimal cross-sensitivity between the two analytes, enabling simultaneous ratiometric imaging of O_2 and pH. The idea of multianalyte imaging is not new,[17,35,36] and several systems have been proposed and in part applied to measure "real world" samples.[37] Nevertheless, many of these systems use expensive cameras (lifetime based imaging),[27] multiple excitation sources or optical filter combinations, which results in complex imaging systems. In this study, we showed that a simple system consisting of a single camera, a single excitation source, and a single filter can be used to enable dual-analyte imaging of O_2 and pH. The system takes advantage of a camera that houses 2 CCDs.[17] While one of them is a "standard" color chip (RGB) the second one is solely sensitive to near-infrared radiation (NIR). The spectral sensitivities of the 2 CCDs are depicted in Figure 1B. It can be observed that the NIR channel is completely separated from the other channels. In contrast, the blue, green, and red channels show substantial overlap, a common limitation when using RGB cameras. In order to develop a sensor without cross-sensitivity those overlaps have to be considered. In the following the rationale behind the sensor design is explained.

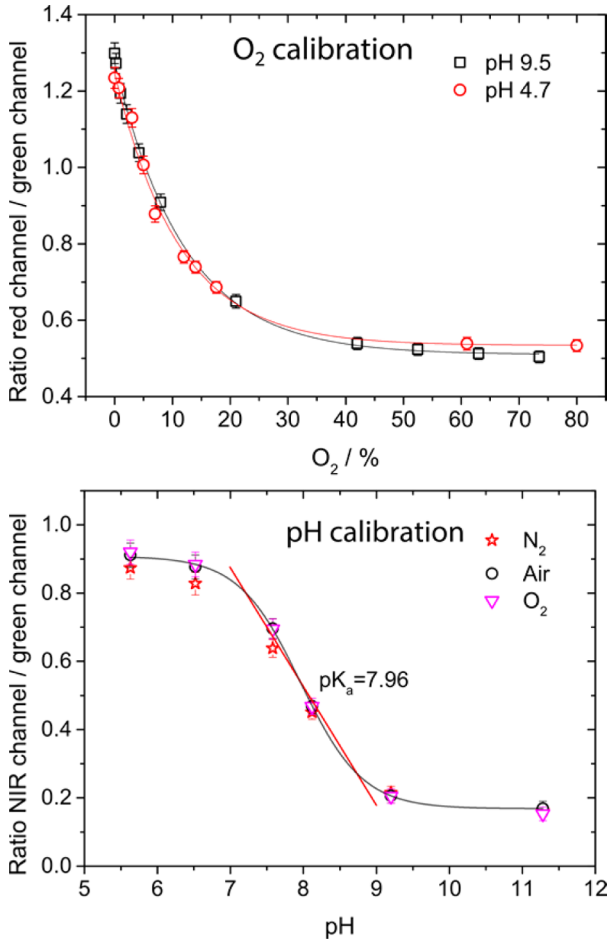

Figure 2. Calibration plots for O_2 and pH for the new dual sensor. Both plots were obtained at varying concentrations of the respective other analyte. In the pH calibration, a slight cross-sensitivity to O_2 can be observed at pH values < pK_a. The red line in the pH calibration represents a linear fit within the image analysis program. Points represent mean values (±SD) obtained from the entire imaged sensor.

Dyes. The dual sensor was optimized in order to minimize spectral overlap and subsequent cross-sensitivity. Additionally, photostability and adequate sensitivity of the indicators were important factors when designing the sensor. The chosen pH indicator OHButoxy-aza-BODIPY is highly photostable[28] and its emission falls fairly well in the NIR channel of the 2CCD camera system. Preliminary investigations based on the commonly used O_2 sensitive dye platinum(II)-5,10,15,20-tetrakis(2,3,4,5,6-pentafluorphenyl)-porphyrin (PtTFPP) in combination with the OHButoxy-aza-BODIPY dye showed

DOI: 10.1021/acssensors.6b00071
ACS Sens. 2016, 1, 681–687

strong cross-sensitivities in the O_2 calibration (due to an overlap of the emission of PtTFPP (λ_{max} 650 nm) with the pH-dependent absorption of the aza-BODIPY resulting in a pH-modulated inner-filter effect) as well as in the pH calibration (due to the emission shoulder of PtTFPP in the NIR region). Spectra of the sensor containing PtTFPP as well as the respective calibration curves can be found in the Supporting Information (Figures S6 and S7). In contrast, O_2 indicators based on Eu(III) complexes did not produce cross-talk due to their very narrow emission (fwhm ≈ 4 nm) peaking at 613−617 nm. While virtually all Eu(III) complexes show insufficient sensitivity to O_2, a recently reported hydroxyphenalenone complex Eu(HPhN)$_3$dpp[29] represents a notable exception. Moreover, this complex is excitable in the blue part of the spectrum, which is particularly attractive for the design of a dual sensor system. A new Bu_3Coum dye was chosen as reference dye due to its distinct emission in the green region and high lipophilicity, which prevents its migration into the more hydrophilic hydrogel from the hydrophobic polystyrene. Spectra of all the dyes and their overlap with the 4 color channels of the 2CCD camera system can be found in Figure 1B. All the dyes used can be excited in the blue part of the spectrum (400−470 nm). A common excitation is beneficial as it minimizes the equipment needed (single LED). Additionally, in this specific dye arrangement only a single filter (long pass filter OG510) is required to block the excitation light from reaching the camera.

Sensor System. Besides the adjustment of the optical properties of the dyes relative to each other and the camera channel, respectively, it was also important to immobilize the selected dyes in an appropriate matrix. While O_2 indicators are commonly immobilized in hydrophobic polymers,[22] pH indicators need to be exposed to water and demand a hydrophilic matrix. Additional components of the sensor encompassed a signal enhancing layer[38] improving the optical signals due to enhanced light scattering and an optical isolation layer[39] for blocking background light (e.g., from chlorophyll fluorescence, a common source of fluorescence in photosynthetic systems as shown in Figure 3).

The developed sensor system consists of three layers. The layer closest to the transparent sensor support (polyethylene terephthalate) is a polystyrene (PS) layer incorporating the O_2 sensitive Eu(HPhN)$_3$dpp dye as well as the Bu_3Coum reference dye. The second layer is a D4 hydrogel containing the OHButoxy-aza-BODIPY and diamond powder. The latter layer combines pH sensing as well as signal enhancing properties due to the diamond powder. Diamond powder was chosen over the frequently used TiO_2[38] to avoid its potentially interfering photocatalytic properties. In comparison to SiO_2 (n = 1.4585), the refractive index of diamond powder (n = 2.42) is significantly higher which makes it more attractive to use for scattering enhancement of optical signals. Additionally adding diamond powder increased the adhesion between the layers and has a lower refractive index than TiO_2. A further D4 hydrogel layer consisting of the pH sensitive OHButoxy-aza-BODIPY dye and carbon black was included to eliminate background light interferences; the pH sensitive dye was added to the optical isolation layer to avoid dye migration and thus changes in the signal intensities. The optical isolation was chosen to be of the same thickness as the pH layer to ensure complete blocking of background light including potentially interfering chlorophyll fluorescence signals from the densely pigmented biofilm. Although the optical isolation layer contains the pH indicator, it has to be noted that the indicator was only added to avoid dye migration between the layers. The pH dependent emission was only detected from the underlying pH sensitive layer as the black isolation absorbs all the emission of the pH indicator within the optical isolation.

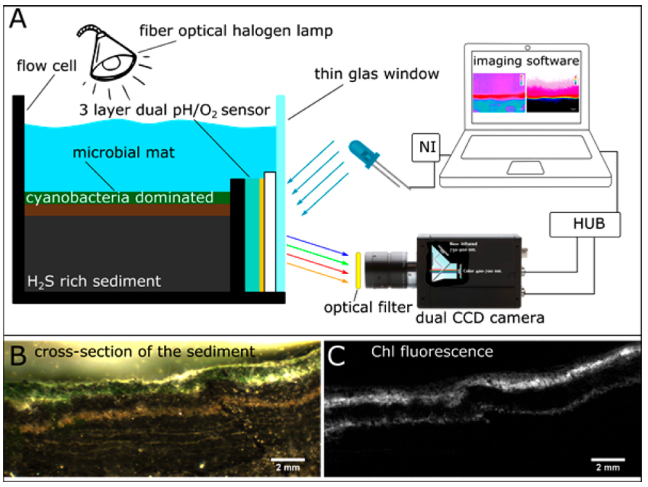

Figure 3. (A) Visualization of the used imaging system. A flow cell with a glass window was constructed and used to study O_2 and pH dynamics in a microbial mat that was freshly cut and pressed against the dual sensor. Image acquisition and triggering of the LED was controlled by the imaging software. (B) Cross-section of the microbial mat and the sediment core, as seen through the glass window without the sensor foil. (C) Chlorophyll fluorescence in the microbial mat due to 405 nm excitation visible in the NIR channel of the camera.

Sensor Calibration and Evaluation of Cross-Sensitivity. In order to evaluate potential cross-talk calibrations for O_2 and pH were conducted at varying concentrations of the other respective analyte. Stepwise changes in the O_2 concentration were conducted for two pH values: one acidic and one alkaline (Figure 2). For the other pH values, only air saturation, 100% and 0% O_2 were measured. The obtained values at intermediate pH values fell well within the obtained calibration (not shown in Figure 2). The O_2 calibration showed no cross interferences caused by changes in the pH and exhibited a dynamic range between 0% and 40% O_2, although with strongly reduced sensitivity between 20% and 40% O_2. Such low sensitivity at higher O_2 levels was expected for Eu(HPhN)$_3$dpp due to the rather long decay time (350 μs)[29] of this dye. As O_2 sensitivity of an optical O_2 sensor is mainly influenced by the decay time of the indicator and the O_2 permeability of the polymer, further tuning of the sensitivity can be achieved by changing the polymer matrix[40] without interfering with the spectral properties of the sensor materials.

The pH response of the dual sensor followed a sigmoidal pattern with an apparent pK_a of around 7.96. A minor cross-sensitivity toward O_2 was observed at pH values beneath the pK_a (Figure 2). This can be explained by the spectral overlap of the red and green channels of the camera. A decrease of O_2 results in an increase in the emission of the O_2 indicator seen predominantly in the red channel. Due to the slight spectral overlap there are subsequently minor increases in the green channel, resulting in lower NIR/G ratio values. However, for most applications, this minor cross-sensitivity between the two analytes is not problematic and lies well within the experimental error. Due to practical reasons (image analysis) the sigmoidal calibration curve was approximated using a linear fit, as the

DOI: 10.1021/acssensors.6b00071
ACS Sens. 2016, 1, 681−687

sigmoidal curve was almost perfectly linear over a range of ±0.5 pH units around the pK_a (Figure 2). In order to maximize the possible dynamic range of the sensor, a range of ±1 pH units around the pK_a was chosen. Although the linear approximation deviates from the correct sigmoidal fit, especially at pH values <7.2 and >8.8, the sample used showed (Figure 4) a minimal

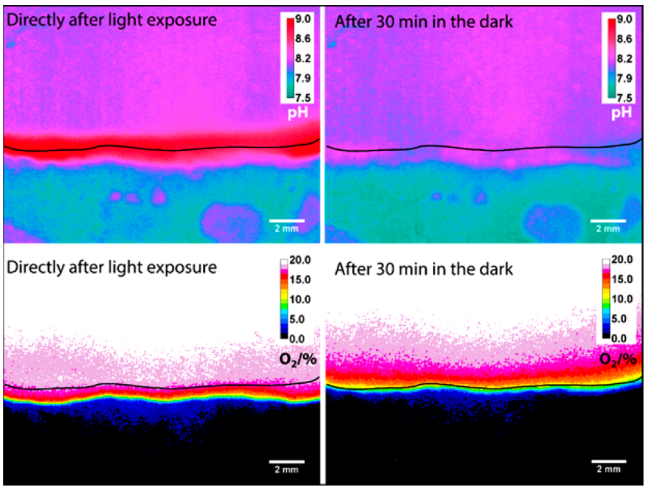

Figure 4. Calibrated false color pH (top) and O_2 (bottom) images of the studied microbial mat directly after light exposure (330 μmol photons m^{-2} s^{-1}) and after 30 min in the dark. The surface of the mat is represented by the black line.

pH value in the sediment of approximately 7.5, which is located in the linear range of the curve and a maximal pH value in the surface layer of approximately 9, which is in accordance with additionally conducted microsensor profiling (see Supporting Information). The linear fit thus proved sufficient for this sample and we note that the cross-sensitivity toward O_2 has a smaller effect on accuracy of the sensor reading than the applied linear fit. For samples covering a broader pH range, a broad range pH sensor system would be required, which consists of multiple pH indicators dyes.[28] In this case a linear fit would not be adequate and more complicated processing algorithms would be necessary.

Besides sensor calibration, the sensor response time is another important characteristic determining at which time scale measurements can be conducted. The response time of the dual sensor (t_{90}) was <20 s for both analytes (see Figure S10). This is in good agreement with literature values for sensors of similar thickness.[16] Thus, the measurements of the dynamics in the microbial mats were conducted in 30 s time steps.

Application of the Dual-Sensor for Imaging O_2 and pH Simultaneously within a Microbial Mat. In order to test the applicability of the dual sensor on a real world sample, sediment cores with a distinct microbial mat at the surface layer were collected and analyzed. A fresh cut sediment core was pressed against the dual sensor and illuminated with an external light source until steady state was reached (see setup in Figure 3). After the external illumination was switched off, images were acquired continuously for 30 min. Although it was attempted to firmly press the sample against the sensor, the rather sandy consistency of the sample complicated that. In the case of muddier sediments or samples, close contact of the sensor and the sample can be achieved more easily.

Images of the 2D O_2 and pH distribution in the microbial mat recorded directly after light exposure and after 30 min in the dark are shown in Figure 4. The surface of the microbial mat is depicted as a black line. For both analytes, distinct differences were observed between light and dark conditions. As the cyanobacteria present in the microbial mat are capable of performing photosynthesis, images recorded directly after light exposure showed increased O_2 concentration and pH values close to the surface of the mat. After light exposure, the pH around the microbial mat surface increased by up to 0.8 pH units relative to the seawater pH due to CO_2 fixation by cyanobacterial photosynthesis. In contrast, the pH image recorded after 30 min in darkness showed that pH at the microbial mat surface was similar to pH in the overlaying seawater. Surprisingly, no particularly high O_2 oversaturation was observed after light exposure and this can be explained by (i) a lack in sensitivity of the O_2 sensor above air saturation and (ii) a possibly nonideal contact between the sample and the sensor. Nevertheless, this shows that it is important to adapt the used sensor to the analytical problem. The pH sensor on the other hand exhibited a perfect dynamic range for the processes observed in the microbial mat.

To analyze the pH and O_2 dynamics of the system in more detail, three different areas of interest with equal sizes were selected (see Figure 5). One was chosen to be exposed to the

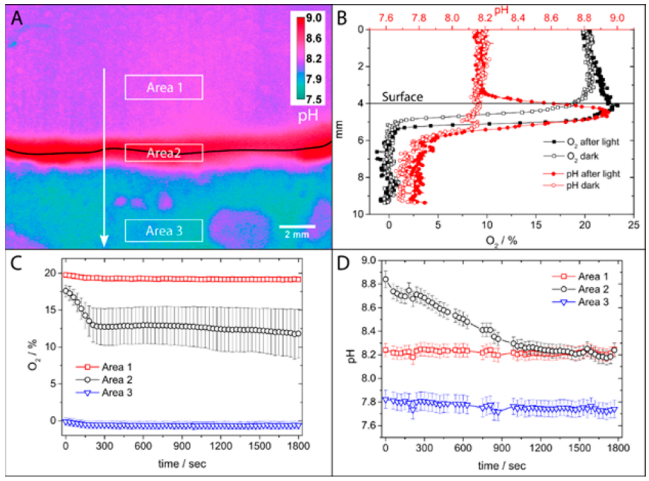

Figure 5. Extraction of time-resolved and depth-resolved dynamics from recorded O_2 and pH images. (A) The arrow indicates where vertical O_2 and pH profiles shown in panel B where extracted. Boxes visualize specific areas of interest. (B) pH (red) and O_2 (black) profiles directly after light exposure (full symbols) and after a 30 min dark period (open symbols). (C) Changes in O_2 concentration over time in the three selected areas. (D) Changes in the pH over time in the three selected areas.

seawater above the microbial mat (area 1) exhibiting seawater pH and full air saturation, the second area crossed the mat–water interface (area 2), while the third area was exposed to deeper sediment layers (area 3) exhibiting approximately pH 7.8 and anoxic conditions. The changes in O_2 concentrations and pH in areas 1 and 3 are, as expected, negligible over time, while the most drastic changes occurred in area 2, i.e., around the biofilm–water interface (Figure 5C and D). Decreasing O_2 concentration and pH were observed in the latter zone immediately after the light was switched off. While the O_2 concentration reached equilibrium within the first 5 min in

DOI: 10.1021/acssensors.6b00071
ACS Sens. 2016, 1, 681–687

darkness, the change in pH from 8.8 to 8.2, i.e., the pH of the seawater, took place much more slowly and was only completed after 20 min reflecting the balance of different microbial metabolic processes within the microbial mat.[32] The new dual sensor thus allows the investigation of pH and O_2 dynamics of the exact same area which was subject to identical pretreatment.

Besides mapping of time dependent changes of the two analytes, concentration profiles through the sample can be extracted from the chemical images (Figure 5A,B). A set of vertical depth profiles of O_2 concentration and pH just after illumination and after 30 min in darkness is shown in Figure 5B. The pH profiles showed a distinct pH maximum just beneath the mat surface that disappeared during the dark period. A slight O_2 maximum at the mat surface was seen just after darkening, but due to the previously described sensor dynamics the measurement accuracy was restricted. Nevertheless, the O_2 measurement revealed that the oxic zone increased dramatically due to photosynthetic activity of the mat. Similar dynamics were observed when using commercial microsensors (see Figure S11).

CONCLUSION

A novel dual sensor system for the simultaneous, low-cost imaging of O_2 concentrations and pH was developed and tested on microbial mats. The novel indicator dye was chosen due to its excitability in the blue part of the spectrum and emission in the green region, as well as its high lipophilicity. The O_2 sensitive indicator was selected for its narrow emission peak in the red region, which minimizes cross-talk between the channels, its good O_2 sensitivity in comparison to other Eu(III) dyes, and its excitability in the blue region. The pH sensitive dye was chosen due to its emission in the NIR part of the spectrum and its high photostability. The system was optimized toward minimal cross-sensitivity between the two analytes, maximal signal intensity by the introduction of a signal-enhancing scattering layer utilizing diamond powder, and the blocking of background interferences by the introduction of an additional optical isolation layer. It was possible to simultaneously visualize dynamic changes in pH and O_2 concentration as a function of irradiance in dense microbial mats exhibiting high background fluorescence.

The sensor system is easy to use, cheap, and allows real time monitoring of dynamic processes within a pH range from 7 to 9 and O_2 concentration between 0% and up to 40% (albeit with limited resolution above 20%). These specific properties make this dual sensor system suitable for a broad field of environmental applications[41] or process monitoring.

ASSOCIATED CONTENT

Supporting Information

The Supporting Information is available free of charge on the ACS Publications website at DOI: 10.1021/acssensors.6b00071.

NMR spectra of the synthesized Bu_3Coum, calibration plots of a sensor system using a nonideal dye combination, pictures of the experimental setup and environmental samples, and microsensor profiles measured in the microbial mat (PDF)

AUTHOR INFORMATION

Corresponding Authors

*E-mail: klaus.koren@bio.ku.dk.

*E-mail: sergey.borisov@tugraz.at.

Author Contributions

M.S. and S.M.B. synthesized the used dyes. M.M., I.K., and S.M.B. designed the dual analyte sensor. M.K. and K.K. designed the biological measurements that were performed by M.M. and K.K. The manuscript was written by M.M. with contributions from all authors. All authors have given approval to the final version of the manuscript.

Notes

The authors declare no competing financial interest.

ACKNOWLEDGMENTS

This study was supported by grants from the Villum Foundation (K.K., M.K.), Erasmus+ (M.M.), European Commission (M.M., S.M.B., Project SenseOcean, Grant Agreement Number 614141); MS, FP7 Project BIOINTENSE, Grant Agreement Number 312148), the Danish Research Council for Independent Research | Technology and Production Sciences (K.K., M.K.), and by a Sapere-Aude Advanced grant from the Danish Council for Independent Research | Natural Sciences (M.K.). We thank Sofie L. Jakobsen and Egil Nielsen for technical assistance, and Nick Blackburn (Bioras Aps) for developing the imaging software and trigger device for the new imaging system. Christoph Staudinger is thanked for helping with image analysis and for fruitful discussions.

REFERENCES

(1) McDonagh, C.; Burke, C. S.; MacCraith, B. D. Optical chemical sensors. *Chem. Rev.* **2008**, *108*, 400−422.

(2) Schäferling, M. The art of fluorescence imaging with chemical sensors. *Angew. Chem., Int. Ed.* **2012**, *51*, 3532−3554.

(3) Kühl, M. Optical Microsensors for Analysis of Microbial Communities. *Methods Enzymol.* **2005**, *397*, 166−199.

(4) Holst, G.; Grunwald, B. Luminescence lifetime imaging with transparent oxygen optodes. *Sens. Actuators, B* **2001**, *74*, 78−90.

(5) Glud, R. N. Oxygen dynamics of marine sediments. *Mar. Biol. Res.* **2008**, *4*, 243−289.

(6) Polerecky, L.; Volkenborn, N.; Stief, P. High Temporal Resolution Oxygen Imaging in Bioirrigated Sediments. *Environ. Sci. Technol.* **2006**, *40*, 5763−5769.

(7) Santner, J.; Larsen, M.; Kreuzeder, A.; Glud, R. N. Two decades of chemical imaging of solutes in sediments and soils − a review. *Anal. Chim. Acta* **2015**, *878*, 9−42.

(8) Glud, R. N.; Kühl, M.; Kohls, O.; Ramsing, N. B. heterogeneity of oxygen production and consumption in a photosynthetic microbial mat as studied by planar optodes. *J. Phycol.* **1999**, *35*, 270−279.

(9) Jovanovic, Z.; Pedersen, M.; Larsen, M.; Kristensen, E.; Glud, R. Rhizosphere O2 dynamics in young Zostera marina and Ruppia maritima. *Mar. Ecol.: Prog. Ser.* **2015**, *518*, 95−105.

(10) Frederiksen, M. S.; Glud, R. N. Oxygen dynamics in the rhizosphere of Zostera marina: A two-dimensional planar optode study. *Limnol. Oceanogr.* **2006**, *51*, 1072−1083.

(11) Kühl, M.; Behrendt, L.; Trampe, E.; Qvortrup, K.; Schreiber, U.; Borisov, S. M.; Klimant, I.; Larkum, A. W. D. Microenvironmental Ecology of the Chlorophyll b-Containing Symbiotic Cyanobacterium Prochloron in the Didemnid Ascidian Lissoclinum patella. *Front. Microbiol.* **2012**, *3*, 402.

(12) Staal, M.; Borisov, S. M.; Rickelt, L. F.; Klimant, I.; Kühl, M. Ultrabright planar optodes for luminescence life-time based microscopic imaging of O2 dynamics in biofilms. *J. Microbiol. Methods* **2011**, *85*, 67−74.

(13) Lu, H.; Jin, Y.; Tian, Y.; Zhang, W.; Holl, M. R.; Meldrum, D. R. New ratiometric optical oxygen and pH dual sensors with three emission colors for measuring photosynthetic activity in Cyanobacteria. *J. Mater. Chem.* **2011**, *21*, 19293−192301.

DOI: 10.1021/acssensors.6b00071
ACS Sens. 2016, 1, 681−687

(14) Rudolph-Mohr, N.; Vontobel, P.; Oswald, S. E. A multi-imaging approach to study the root-soil interface. *Ann. Bot.* **2014**, *114*, 1779−1787.
(15) Zhu, Q.; Aller, R. C. Planar fluorescence sensors for two-dimensional measurements of H2S distributions and dynamics in sedimentary deposits. *Mar. Chem.* **2013**, *157*, 49−58.
(16) Larsen, M.; Borisov, S. M.; Grunwald, B.; Klimant, I.; Glud, R. N. A simple and inexpensive high resolution color ratiometric planar optode imaging approach: application to oxygen and pH sensing. *Limnol. Oceanogr.: Methods* **2011**, *9*, 348−360.
(17) Ehgartner, J.; Wiltsche, H.; Borisov, S. M.; Mayr, T. Low cost referenced luminescent imaging of oxygen and pH with a 2-CCD colour near infrared camera. *Analyst* **2014**, *139*, 4924−4933.
(18) Ungerböck, B.; Charwat, V.; Ertl, P.; Mayr, T. Microfluidic oxygen imaging using integrated optical sensor layers and a color camera. *Lab Chip* **2013**, *13*, 1593−1601.
(19) Schreml, S.; Meier, R. J.; Wolfbeis, O. S.; Landthaler, M.; Szeimies, R.-M.; Babilas, P. 2D luminescence imaging of pH in vivo. *Proc. Natl. Acad. Sci. U. S. A.* **2011**, *108*, 2432−2437.
(20) Dmitriev, R. I.; Kondrashina, A. V.; Koren, K.; Klimant, I.; Zhdanov, A. V.; Pakan, J. M. P.; McDermott, K. W.; Papkovsky, D. B. Small molecule phosphorescent probes for O2 imaging in 3D tissue models. *Biomater. Sci.* **2014**, *2*, 853.
(21) Fercher, A.; Borisov, S. M.; Zhdanov, A. V.; Klimant, I.; Papkovsky, D. B. Intracellular O2 sensing probe based on cell-penetrating phosphorescent nanoparticles. *ACS Nano* **2011**, *5*, 5499−5508.
(22) Wang, X.-D.; Wolfbeis, O. S. Optical methods for sensing and imaging oxygen: materials, spectroscopies and applications. *Chem. Soc. Rev.* **2014**, *43*, 3666−3761.
(23) Meier, R. J.; Fischer, L. H.; Wolfbeis, O. S.; Schäferling, M. Referenced luminescent sensing and imaging with digital color cameras: A comparative study. *Sens. Actuators, B* **2013**, *177*, 500−506.
(24) Koren, K.; Kühl, M. A simple laminated paper-based sensor for temperature sensing and imaging. *Sens. Actuators, B* **2015**, *210*, 124−128.
(25) Wang, X.; Stolwijk, J. A.; Lang, T.; Sperber, M.; Meier, R. J.; Wegener, J.; Wolfbeis, O. S. Ultra-small, highly stable, and sensitive dual nanosensors for imaging intracellular oxygen and pH in cytosol. *J. Am. Chem. Soc.* **2012**, *134*, 17011−17014.
(26) Wencel, D.; Abel, T.; McDonagh, C. Optical chemical pH sensors. *Anal. Chem.* **2014**, *86*, 15−29.
(27) Borisov, S. M.; Vasylevska, A. S.; Krause, C.; Wolfbeis, O. S. Composite Luminescent Material for Dual Sensing of Oxygen and Temperature. *Adv. Funct. Mater.* **2006**, *16*, 1536−1542.
(28) Strobl, M.; Rappitsch, T.; Borisov, S. M.; Mayr, T.; Klimant, I. NIR-emitting aza-BODIPY dyes - new building blocks for broad-range optical pH sensors. *Analyst* **2015**, *140*, 7150−7153.
(29) Borisov, S. M.; Fischer, R.; Saf, R.; Klimant, I. Exceptional Oxygen Sensing Properties of New Blue Light-Excitable Highly Luminescent Europium(III) and Gadolinium(III) Complexes. *Adv. Funct. Mater.* **2014**, *24*, 6548−6560.
(30) Christie, R. M.; Lui, C.-H. Studies of fluorescent dyes: part 2. An investigation of the synthesis and electronic spectral properties of substituted 3-(2′-benzimidazolyl)coumarins. *Dyes Pigm.* **2000**, *47*, 79−89.
(31) Tsatsaroni, E. G.; Peters, a T.; Lin, S. M. Synthesis and characterisation of 3-ketocoumarins: substituent effects on colour. *Color. Technol.* **1999**, *115*, 62−68.
(32) Nielsen, M.; Larsen, L. H.; Ottosen, L. D. M.; Revsbech, N. P. Hydrogen microsensors with hydrogen sulfide traps. *Sens. Actuators, B* **2015**, *215*, 1−8.
(33) Lassen, C.; Ploug, H.; Jørgensen, B.; Jmgensen, B. B. Microalgal photosynthesis and spectral scalar irradiance in coastal marine sediments of Limfjorden, Denmark. *Limnol. Oceanogr.* **1992**, *37*, 760−772.
(34) Ploug, H.; Lassen, C.; Jcrgensen, B. B. Action spectra of microalgal photosynthesis and depth distribution of spectral scalar irradiance in a coastal marine sediment of Limfjorden, Denmark o. *FEMS Microbiol. Ecol.* **1993**, *12*, 69−78.
(35) Stich, M. I. J.; Fischer, L. H.; Wolfbeis, O. S. Multiple fluorescent chemical sensing and imaging. *Chem. Soc. Rev.* **2010**, *39*, 3102.
(36) Meier, R. J.; Schreml, S.; Wang, X.; Landthaler, M.; Babilas, P.; Wolfbeis, O. S. Simultaneous Photographing of Oxygen and pH In Vivo Using Sensor Films. *Angew. Chem., Int. Ed.* **2011**, *50*, 10893−10896.
(37) Schreml, S.; Meier, R. J.; Kirschbaum, M.; Kong, S. C.; Gehmert, S.; Felthaus, O.; Küchler, S.; Sharpe, J. R.; Wöltje, K.; Weiß, K. T.; et al. Luminescent dual sensors reveal extracellular pH-gradients and hypoxia on chronic wounds that disrupt epidermal repair. *Theranostics* **2014**, *4*, 721−735.
(38) Glud, R.; Ramsing, N.; Gundersen, J. K.; Klimant, I. Planar optrodes: a new tool for fine scale measurements of two-dimensional O2 distribution in benthic communities. *Mar. Ecol.: Prog. Ser.* **1996**, *140*, 217−226.
(39) Klimant, I.; Kühl, M.; Glud, R. N.; Holst, G. Optical measurement of oxygen and temperature in microscale: strategies and biological applications. *Sens. Actuators, B* **1997**, *38*, 29−37.
(40) Koren, K.; Hutter, L.; Enko, B.; Pein, A.; Borisov, S. M.; Klimant, I. Tuning the dynamic range and sensitivity of optical oxygen-sensors by employing differently substituted polystyrene-derivatives. *Sens. Actuators, B* **2013**, *176*, 344−350.
(41) Glud, R. N.; Wenzhöfer, F.; Tengberg, A.; Middelboe, M.; Oguri, K.; Kitazato, H. Distribution of oxygen in surface sediments from central Sagami Bay, Japan: In situ measurements by micro-electrodes and planar optodes. *Deep Sea Res., Part I* **2005**, *52*, 1974−1987.

DOI: 10.1021/acssensors.6b00071
ACS Sens. 2016, 1, 681−687